Available online at www.sciencedirect.com
SCIENCE DIRECT®
International Journal of Heat and Mass Transfer 49 (2006) 4200–4208
International Journal of HEAT and MASS TRANSFER
www.elsevier.com/locate/ijhmt

# The effect of gap distance on the heat transfer between a heated finned surface and a saturated porous plate

M.J. Schertzer, D. Ewing, C.Y. Ching *

*Department of Mechanical Engineering, McMaster University, Hamilton, Ont., Canada L9G 4Z5*

Received 9 November 2005; received in revised form 10 March 2006
Available online 22 May 2006

**Abstract**

Experiments were performed to investigate the effect that the presence of a gap has on the heat transfer between a heated finned surface and a saturated porous plate with an average pore radius of 200 μm. There was evidence that the vapour generated beneath the heated surface can escape to the vapour grooves more easily when a gap distance is introduced. This seemed to decrease the vapour penetration into the porous plate. The heat transfer performance of the heated finned surface initially increased as the gap distance was increased from 0 to 500 μm, but remained relatively unchanged for gap distances of 500–900 μm.


*Keywords:* Boiling; Porous structure; Two phase heat transfer; Capillary evaporator

## 1. Introduction

There is an increasing demand for highly effective heat transport systems due to increasing heat flux requirements and thermal constraints in many applications, including electronics cooling and heat transport systems in space applications [1–3]. There has been interest in using passive two phase heat transport devices, such as heat pipes and capillary pumped loops (CPLs), to meet this demand because they can provide relatively isothermal heat removal even at high heat fluxes. Many of the passive two phase heat transfer devices use the capillary force developed in a porous wick to circulate a working fluid, and thus do not rely on mechanical components. The heat is transferred to the working fluid in the porous wick at the evaporator, so at high heat fluxes the boiling process in the evaporator can limit the wicking of the fluid in the porous media, and lead to failure of the device.

In capillary pumped loops, the heat is transferred to the liquid in the porous wick through a series of heated fins. The vapour generated from the evaporated liquid must then escape to vapour grooves between the heated fins that lead to the vapour line exiting the evaporator section [4]. A number of numerical models have been developed to estimate both the heat transfer from a heated fin to a saturated porous structure and the liquid vapour interface within the porous structure by solving the momentum and energy equations. The most basic of these models assumed that any vapour penetration into the wick would have a detrimental effect on evaporator performance [5,6], while other models assumed that the evaporator could maintain stable operation with vapour present within the porous structure. The vapour penetration in these models is typically treated as a one dimensional [7,8] or two dimensional [9] single phase vapour region, or a two phase flow regime. Most of these models predicted that the vapour penetration into the wick would increase with heat flux, leading to a decrease in the heat transfer performance. Indeed, experimental measurements of capillary evaporators suggest that the heat transfer coefficient remains constant at low to moderate heat fluxes, but decreases at high heat fluxes [10].

* Corresponding author. Tel.: +1 905 525 9140x24998; fax: +1 905 572 7944.
*E-mail address:* chingcy@mcmaster.ca (C.Y. Ching).

0017-9310/$ - see front matter © 2006 Elsevier Ltd. All rights reserved.
doi:10.1016/j.ijheatmasstransfer.2006.03.020

**Nomenclature**

| | |
|---|---|
| $C_P$ | specific heat (J/kg K) |
| $d$ | depth beneath the upper surface of the porous plate (m) |
| $G$ | gap distance between the heated surface and the porous plate (m) |
| $h$ | average heat transfer coefficient (W/m$^2$ K) |
| $h_{fg}$ | enthalpy of evaporation (J/kg) |
| $I$ | current through the resistive foil (A) |
| $k_v$ | effective thermal conductivity of the porous plate (W/m K) |
| $\dot{m}$ | mass flow rate pumped by the wick (kg/s) |
| $q''$ | heat flux (W/m$^2$) |
| $Q$ | heat transfer rate (W) |
| $t$ | time (s) |
| $T$ | temperature (K) |
| $V$ | total voltage drop across copper electrodes (V) |
| $w$ | spanwise position from the centre of the heated foil (m) |
| $\alpha$ | thermal diffusivity (m$^2$/s) |
| $\varepsilon$ | emissivity of the heating surface |
| $\Phi$ | porosity of the porous plate |

*Subscripts*

| | |
|---|---|
| Elec | electrical heating |
| Loss | heat lost to the ambient |
| W | wick |
| Sur | heated surface |
| Sat | saturation |
| Sub | subcooled |

The formation of a two phase liquid–vapour region has been observed experimentally in porous structures of staggered copper cylinders [11] and packed glass beads [12,13] heated from above using a finned copper block. The heat transfer coefficient in these cases initially increased with heat flux to a maximum before decreasing as the heat flux was increased further. The initial increase in the heat transfer performance was attributed to a decrease in the contact angle of the liquid menisci in the porous media as the heat flux increases, while the decrease in the heat transfer coefficient was attributed to the vapour phase locally penetrating into the porous structure, reducing the area available for heat transfer [13].

Figus et al. [14] proposed that introducing a gap between the heated fin and the porous structure would allow the vapour to pass to the channels in the finned surface more easily, reducing the vapour penetration into the wick. Model predictions suggested that gaps as small as 10 μm should improve the heat transfer performance, though measurements for a capillary evaporator with a mean pore size of 20 μm indicated a larger gap of 100 μm yielded the best heat transfer performance [15]. This study also suggested that the optimum gap distance should be greater than the mean pore radius of the porous structure. A poor wick fit, with gap distances of up to 1400 μm, can cause a large decrease in the performance of the evaporator [16], indicating again that there is an optimal gap distance.

The objective of this investigation was to characterize the effect that introducing a gap between a heated finned surface and a porous plate saturated with water has on the heat transfer between the surfaces. The porous plate was heated by a thin resistive stainless steel foil heater attached to a finned block. The heat transfer performance of this system was characterized by examining the temperature on the heated surface, and the temperature distribution within the porous plate. The experimental facility and methodology is described in the next section. The results of the experiments are then presented, and finally the conclusions of the study are outlined.

## 2. Experimental facility

A schematic of the experimental facility used in this investigation is shown in Fig. 1. The facility consists of a main test section that contained the porous plate and the heated finned surface, a constant head tank that supplies preheated working fluid to the test section, and a system reservoir. The water from the system reservoir was continually pumped into the constant head tank, and allowed to overflow back into the reservoir in a controlled manner to maintain the height of the fluid in the constant head tank. The height was adjusted so that the water level was at the same height as the top of the porous plate in the main test section in the experiments reported here. The water in the constant head tank was preheated to 60 °C using a 1 kW plug heater turned on and off using a proportional-integral-derivative (PID) controller with input from a T-type thermocouple located in the tank. The water from the constant head tank entered a small reservoir on the bottom of

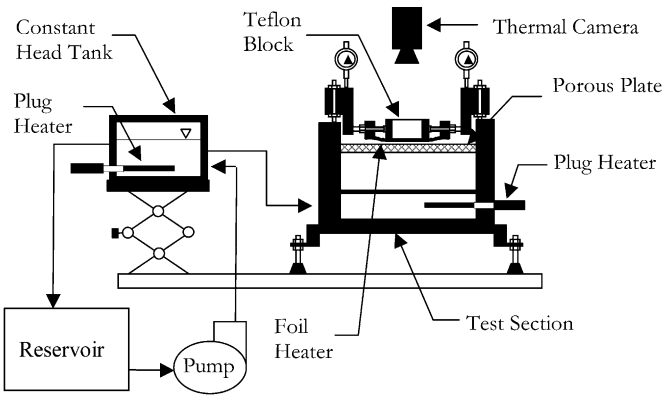


Fig. 1. Schematic of the experimental facility.

the main test section, where it was heated to 75 °C using two 100 W plug heaters turned on and off using a PID controller. The input in this case was the average from five T-type thermocouples placed at various heights in the reservoir. The change in the volume of the working fluid within the system was measured using a graduated cylinder mounted on the system reservoir that was accurate to within ± 2 mL.

The experiments were performed for a 12 mm thick porous alumina plate ($Al_2O_3$) with a reported porosity ($\Phi$) and mean pore radius ($R_P$) of 50% and 200 μm, respectively. This material does not conduct electricity and therefore does not affect the current passing through the resistance heater. The porous plate was positioned on two ledges 150 mm above the bottom of the reservoir in the main test section. The plate was heated from above using a 25 μm thick stainless steel resistive foil that was attached to a machined Teflon block with five 80 mm long fins as shown in Fig. 2. The stainless steel foil had a nominal width of 60 mm, but much of the central portion of the foil was cut away leaving three narrow strips that matched the three central fins of the Teflon block. The middle strip of the foil had a width of 10.0 mm, while the two adjacent strips had widths of 10.5 mm so that the largest heat flux occurred in the central strip. The foil was adhered to the Teflon block using silicon adhesive sealant. The two outermost fins of the Teflon block acted to contain the vapour flow from beneath the two outer heated fins. The 60 mm wide end sections of the stainless steel foil were attached to large copper electrodes that were mounted on rails using Teflon bearings so that the foil could be tensioned after it was heated using adjustable screws. The entire heated finned assembly was mounted on a separate set of rails that could be used to adjust the vertical height of the assembly relative to the porous plate. This distance was measured on either end of the evaporator section using dial gauges with an accuracy of ±12 μm. The uncertainty in the gap distance between the heated foil and the porous plate was less than 30 μm.

The foil was heated using a DC power supply with a maximum current output of 200 A. At steady state, the Joule heating generated within the stainless steel foil is transferred to the working fluid (latent and sensible heating) or lost to the ambient by convection or radiation, so that

$$Q_{elec} = V_T \cdot I = \dot{m} C_P (T_{Sat} - T_{Sub}) + \dot{m} h_{fg} + Q_{Loss}, \quad (1)$$

where $V_T$ is the total voltage drop across the two copper electrodes, $Q_{Loss}$ is the heat lost to the ambient from the heated finned assembly, and $\dot{m}$ is the mass flow rate of water. The voltage drop across the two copper electrodes was measured using an RMS multimeter, while the current was measured with a 50 mV–200 A shunt resistor and a second multimeter. The temperature of the wide sections of the heated foil attached to the copper electrodes was consistently below the saturation temperature of water. Thus, the Joule heating in these sections of the foil was either transferred to the copper electrode, lost to the environment or transferred to the sensible heat of the fluid. The sensible heating of the fluid was however negligible relative to the latent heating of the liquid so the electrical heating in this section was lost to the ambient. Thus, it was assumed that the electrical heating in the thin strips of the foil beneath the fins balanced the latent heating of the water. The heating in the thin strips was estimated using a resistance network, while the latent heating of the water was determined using the mass flow rate from the main reservoir. The heat transfer rate from the latent heating and the electrical heaters agreed to within ±5% in all experiments.

The effect of introducing a gap on the heat transfer between the heated surface and the porous plate was examined in two sets of experiments. In the first set of experiments, the temperature within the porous plate was measured using 0.5 mm diameter T-type thermocouples embedded at different depths spaced 12 mm apart along the length of the porous plate as shown in Fig. 3, and a thermocouple fixed to the underside of the porous plate. The two outermost thermocouples were 15 mm from the ends of the narrow sections of the stainless steel foil. The thermocouples were located within 0.75 mm diameter holes

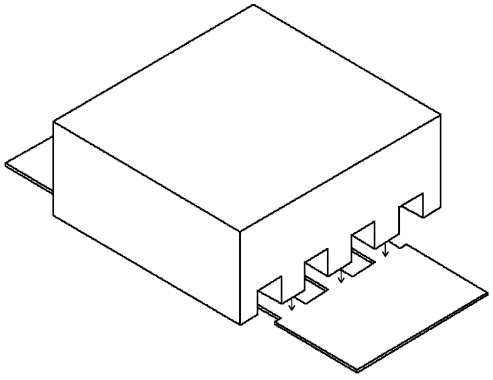

Fig. 2. Sketch showing how the Teflon block is mounted onto the stainless steel foil heater.

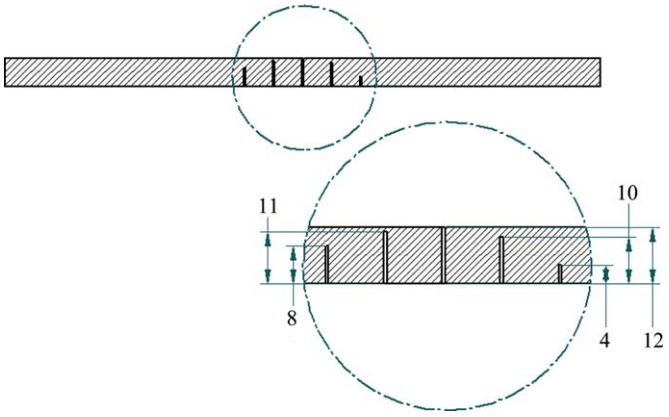


Fig. 3. Sectioned and detailed view of the thermocouple locations within the porous plate. All dimensions in mm.

drilled from the underside of the plate, and fixed in place with silicon rubber adhesive. Care was taken to ensure that the sealant did not coat the tip of the thermocouple or the porous plate. The thermocouples were connected differentially to a 16-channel National Instruments SCB-68 data acquisition board so the bias error in the measurements should be less than 0.2 °C. The six thermocouples were calibrated against a precision RTD with a reported accuracy of 0.014 °C in an oil bath before they were embedded in the porous plate. The temperature profile at different lateral positions below the heated fin were measured by moving the position of the entire instrumented plate laterally using a series of 0.5 mm thick machined stainless steel shims between the edge of the porous plate and the wall of the tank. The uncertainty in the spanwise position due to the uncertainty in the thickness of the shims, and the initial positioning of the plate was approximately 0.7 mm.

The temperature within the porous plate was recorded after the average temperatures within the porous plate remained constant for 5 min. The temperature measurements were recorded at a frequency of 1000 Hz for 30 s. The estimate of the uncertainty in the mean temperature due to the sample size was less than 0.2 °C. The time constants of the thermocouples were evaluated experimentally by immersing a thermocouple in heated water and then removing it. The time constant was approximately 50 ms when it was immersed in the water, but 500 ms when it was removed. Thus, these results suggest that the thermocouple would respond to transients in the liquid temperature but not likely to transients in the vapour temperature on the time scale expected here. The noise in the temperature signal was filtered using a Holt exponential smoothing filter with a coefficient of 0.4 and a characteristic time scale of approximately 4 ms [17].

For the second set of experiments, 5 mm wide grooves were machined through the Teflon block along the centre of the three fins attached to the heated foil. This allowed optical access to the top of the foil so the temperature distribution on the upper surface of the foil heater could be measured using a high-speed infrared camera with a reported accuracy of 1.0 °C and a spatial resolution of approximately 0.5 mm/pixel. The visible portion of the foil was painted with flat black paint that had an emissivity ($\varepsilon$) of $0.96 \pm 0.01$ [18]. The sum of the radiation and convection losses from the exposed portion of the foil were estimated to be approximately 1.2 kW/m$^2$, and it was found the energy balances in these experiments remained within $\pm 5\%$. In each case, 220 thermal images were recorded at both 2 and 60 frames per second after a minimum of 10 min of operation. The uncertainty in the time and space averaged temperature of the foil due to the sample size was less than 0.1 °C. The thermocouples embedded in the porous plate were positioned beneath the centre of the vapour groove in these experiments. An average heat transfer coefficient for the heated fin was determined from the difference between the average foil temperature and the temperature of the liquid below the porous plate. The uncertainty in these heat transfer coefficients was less than 10% at the low heat fluxes, and reduced to less than 6.5% at the high heat fluxes.

The working fluid used in the experiments was distilled water that was degassed by boiling in the constant head tank for 10 min before adding into the test section reservoir. Once the water level was even with the upper surface of the porous plate, it was further degassed by operating the finned heater for 2 h at a heat flux of 30 kW/m$^2$ and a gap distance of 300 μm. The gap distance was then set to zero and the experiments were initiated.

## 3. Results and discussion

Experiments were initially performed with the heated finned surface in contact with the porous plate. The distribution of the time averaged temperature within the porous plate for a heat flux of 15 kW/m$^2$ is presented in Fig. 4. The average temperature in the region beneath the heated fin ($w < 5.0$ mm) is relatively uniform for depths of 0–4 mm. The temperature in the porous plate beneath the vapour groove ($w > 5.0$ mm), however, was much lower. The average temperature beneath the heated surface increased when the heat flux was increased to 25 kW/m$^2$. The change in the temperature with depth in these two cases is compared in Fig. 5. The largest change occurred beneath the centre of the foil ($w = 0$) where the temperatures near the upper surface of the porous plate became relatively independent of depth, suggesting there was vapour present within the porous plate at this location. The average temperature is below the saturation temperature of water, indicating that any vapour present is in a two phase flow, rather than a stable vapour region. The temperature within the porous plate

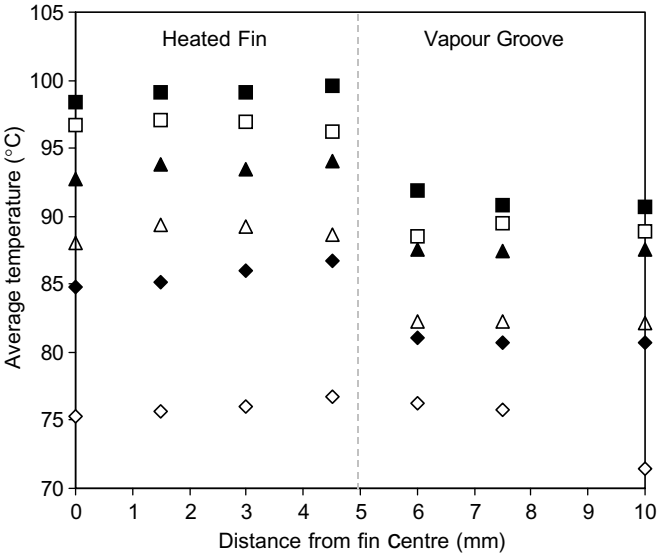


Fig. 4. Spanwise variation of the average temperature in the porous plate at ■ $d = 0$ mm, □ $d = 1$ mm, ▲ $d = 2$ mm, △ $d = 4$ mm, ♦ $d = 8$ mm, ◇ $d = 12$ mm for zero gap distance and a heat flux of 15 kW/m$^2$.

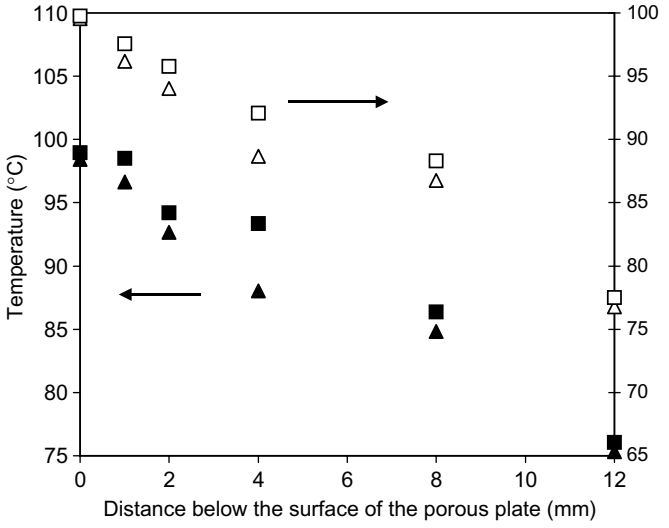


Fig. 5. Change in the average temperature with depth at $w = 0$ mm (solid) and $w = 4.5$ mm (open) for zero gap distance and ▲ $q'' = 15$ kW/m$^2$ and ■ $q'' = 25$ kW/m$^2$.

decreases monotonically with the depth for all heat fluxes, indicating that heat was conducted into the porous plate.

The average temperature of the foil for the zero gap case shown in Fig. 6 remained relatively constant for heat fluxes of 15–20 kW/m$^2$. The temperature increased significantly at a heat flux of 25 kW/m$^2$ due to the presence of persistent high temperature regions on the heated surface. The temperature of the heated foil increased rapidly at higher heat fluxes and did not appear to reach a stable operation. The results for gap distances between 100 and 900 μm, also presented in Fig. 6, show that the introduction of a gap between the heated fin and the porous plate had a significant impact on the heat transfer to the porous media. The change in the average foil temperature with heat flux for the gap distances of 100–300 μm was similar to that when there was no gap. The average temperature of the finned surface with heat flux is non-monotonic for a gap distance of 100 μm, which was smaller than the mean pore size. This may be due to a transition in the boiling dynamics beneath the heated surface. The average temperature of the foil was lower at low heat fluxes when the gap distance was 200 or 300 μm. The maximum heat flux with a stable temperature also increased to 110 kW/m$^2$ when the gap distance was 300 μm. The change in the average foil temperature with heat flux was different when the gap distance was between 500 and 900 μm. In these cases, the average temperature increased gradually with heat flux until a sharp rise in the foil temperature at approximately 210 kW/m$^2$, nearly an order of magnitude higher than the result for the case with no gap. This maximum heat flux seemed independent of gap distance for this range of gap distances. The average foil temperature at heat fluxes higher than this was initially stable but increased rapidly after approximately 90 s suggesting there was a sudden failure in the heat transfer mechanism.

The change in the average heat transfer coefficient for the different gap distances are shown in Fig. 7. In all cases, the heat transfer coefficients increased approximately linearly before reaching a maximum when the average temperature of the foil began to increase. The maximum heat transfer coefficient increased from 0.7 to 7.3 kW/m$^2$ K when the gap was increased from 0 to 500 μm, but was approximately independent of gap distance at the larger gap distances. In CPL applications, the operation of the evaporator is affected by the system pressure drop that was not considered here. This would affect the maximum heat transfer rate and the maximum heat transfer coefficient that could be achieved with stable operation, but likely not the observation that the presence of the gap has a significant impact on the performance of the device.

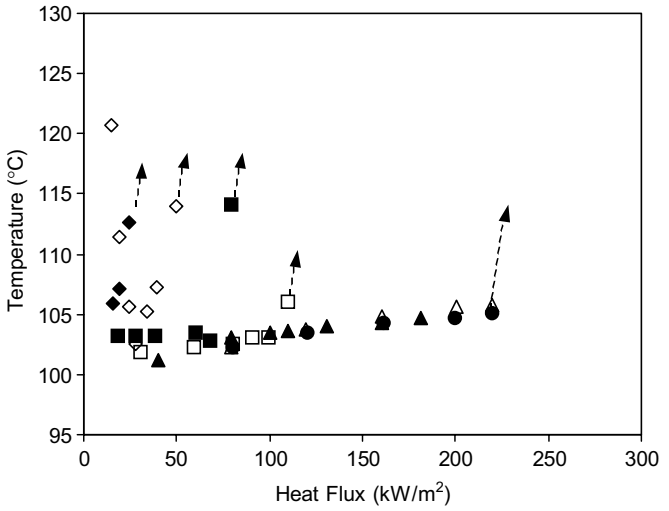


Fig. 6. Change in the time and space averaged foil temperature with heat flux for gap distances of ♦ $G = 0$ μm, ◇ $G = 100$ μm, ■ $G = 200$ μm, □ $G = 300$ μm, ▲ $G = 500$ μm, △ $G = 700$ μm and ● $G = 900$ μm.

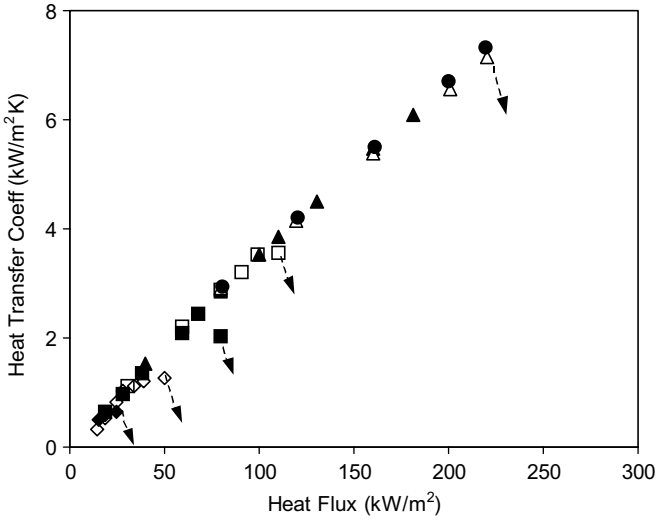


Fig. 7. Change in average heat transfer coefficient with heat flux for gap distances of ♦ $G = 0$ μm, ◇ $G = 100$ μm, ■ $G = 200$ μm, □ $G = 300$ μm, ▲ $G = 500$ μm, △ $G = 700$ μm and ● $G = 900$ μm.

The profiles of the time averaged temperature measured in the porous plate at different heat fluxes when the gap distance was 200 and 500 μm are presented in Fig. 8. The temperature within the porous plate decreases monotonically with depth, similar to the zero gap case. The heat fluxes here are much higher than for the zero gap case, indicating that the presence of the gap did affect the vapour penetration into the porous plate. The temperature beneath the centre of the fin is initially independent of depth when the gap distance is 200 μm, similar to the case with zero gap; however, the temperature is initially more uniform with depth near the edge of the heated foil when the gap was 500 μm. This suggests that there may be more vapour in the porous plate near the edge of the heated fin when the gap is larger. The temperature near the upper surface of the porous plate did not change at these heat fluxes at both the centre and the edge of the heated fin for the 500 μm case, indicating that vapour penetration may be occurring throughout the porous media near the maximum stable heat flux.

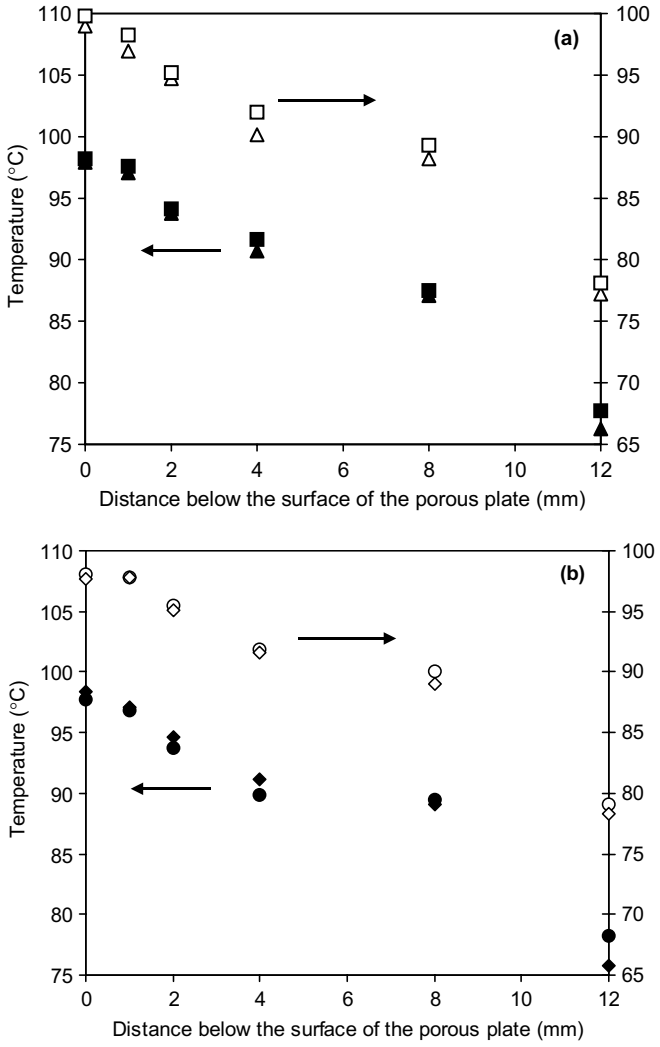


Fig. 8. Variation in the average temperature with depth (a) for gap distance of 200 μm and ■ $q'' = 40$ kW/m$^2$, ▲ $q'' = 80$ kW/m$^2$, and (b) for gap distance of 500 μm and ● $q'' = 120$ kW/m$^2$, ♦ $q'' = 160$ kW/m$^2$. Solid symbols are for $w = 0$ mm and open symbols are for $w = 4.5$ mm.

### 3.1. Boiling dynamics beneath the heated finned surface

The time averaged measurements suggested that the boiling dynamics beneath the heated surface and the vapour penetration into the porous plate changed when a gap was introduced between the heated finned surface and the porous plate. This was examined using the instantaneous measurements of the temperature on the heated surface and within the porous plate. A time sequence of the instantaneous temperature distribution on the heated surface for a heat flux of 15 kW/m$^2$ when no gap was present is shown in Fig. 9. The distributions show spanwise positions between −2 and +2 mm visible to the thermal camera. The temperature on the heated surface was not uniform with regions of temperatures exceeding 110 °C appearing along the centre of the heated surface. These high temperature regions expand and contract with a period of approximately 60 ms, and seem to be the result of vapour regions beneath the heated surface that increase in size until the vapour can travel to the vapour channels. This cyclic behaviour allows stable operation of the heated surface despite the elevated temperatures on the heated surface. The period of the variation of these high temperature regions decreased and the maximum temperature increased when the heat flux was increased to 25 kW/m$^2$, indicating vapour was being trapped under the foil. The growth of these regions likely led to the rapid rise in the temperature of the heated surface when the heat flux was increased further.

Transients of the temperature on the upper surface of the porous plate from the thermocouple measurements at $w = 0$ and 4.5 mm for this case are presented in Fig. 10.

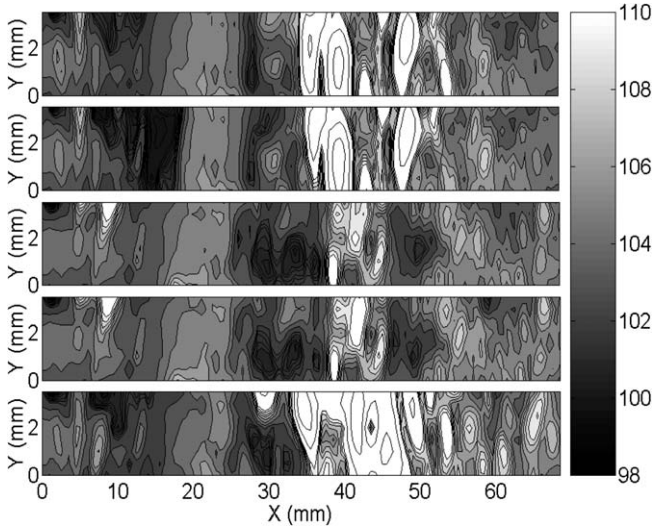


Fig. 9. Transients of the instantaneous temperature distribution (°C) on the heated foil for zero gap distance and a heat flux of 15 kW/m$^2$. These images were recorded 17 ms apart.

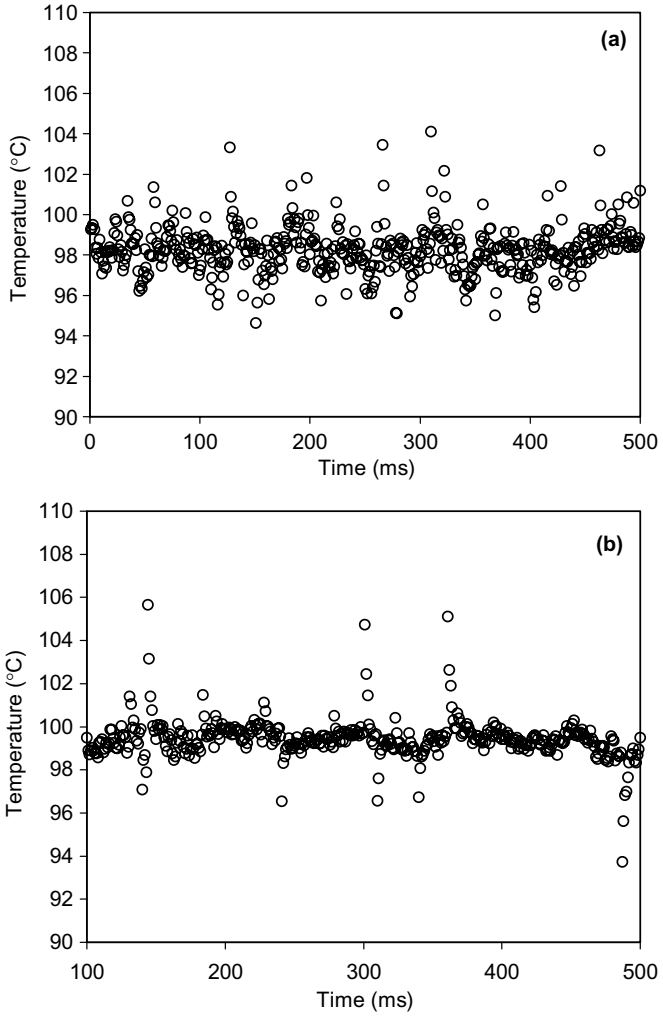


Fig. 10. Transients of the temperature at $d = 0$ mm (the upper surface) of the porous plate at (a) $w = 0$ mm and (b) $w = 4.5$ mm for the zero gap distance and a heat flux of 15 kW/m$^2$.

These time traces were measured in different experiments from each other, so the times in the figures do not correspond. The transients have been filtered but there is still evidence of noise in the signals. The results show though that the temperature fluctuations were more frequent and larger near the center of the foil which is consistent with the suggestion that the vapour periodically built up beneath the centre of the fin before escaping to the vapour groove. The time scale of the fluctuations seemed to be reasonably consistent with those observed in the foil measurements. The frequency and magnitude of the fluctuations increased with heat flux consistent with the measurements of the temperature distributions on the foil. The time traces of the temperature 1 mm beneath the surface of the porous plate for a heat flux of 15 kW/m$^2$ such as that in Fig. 11 showed little variation and the mean temperature was well below saturation. This suggests that there was little or no vapour present at or below this depth.

A typical time series of the instantaneous temperature distributions on the heated foil when the gap distance was 500 μm is shown in Fig. 12. The temperature distribution on the heated foil at the heat flux of 160 kW/m$^2$ (and essentially all heat fluxes for the large gaps), is much more uniform than the temperature distribution when no gap was present. There was also no evidence of high temperature regions on the foil, indicating that the vapour easily escapes to the grooves in the finned surface rather than being trapped beneath the surface. Time traces of the temperature measured at the top of the porous plate for this case are presented in Fig. 13. The temperature fluctuations in this case appear to be more frequent but smaller in magnitude than those observed when no gap was present. The temperature fluctuations are also more frequent and larger towards the edge of the heated fin, suggesting that the void fraction between the heated fin and the porous plate increased along the gap, similar to flow boiling in the channel. There were again few, if any, temperature fluctuations

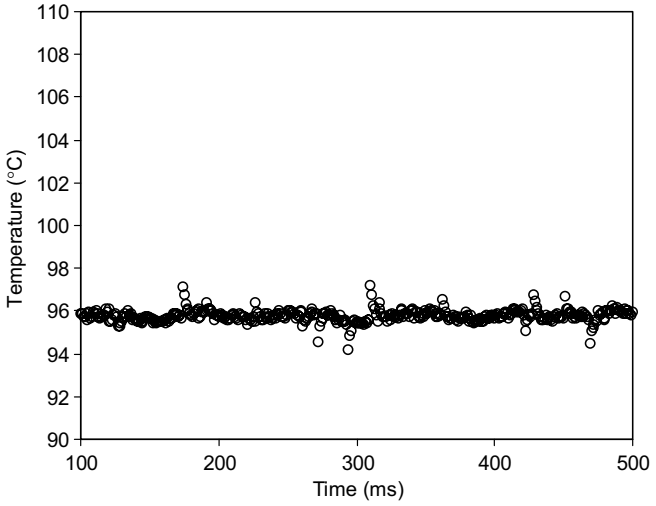


Fig. 11. Transients of the temperature at $d = 1$ mm within the porous plate at $w = 0$ mm for the zero gap distance and a heat flux of 15 kW/m$^2$.

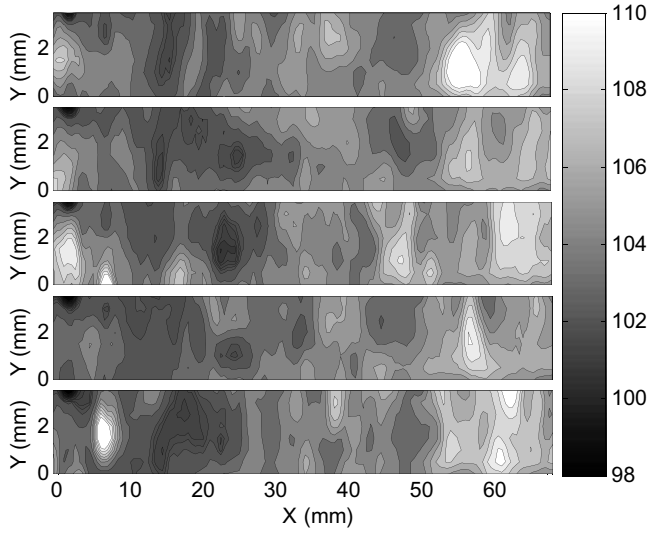


Fig. 12. Transients of the instantaneous temperature distributions (°C) on the heated foil for a gap distance of 500 μm and a heat flux of 160 kW/m$^2$. These images were recorded 17 ms apart.

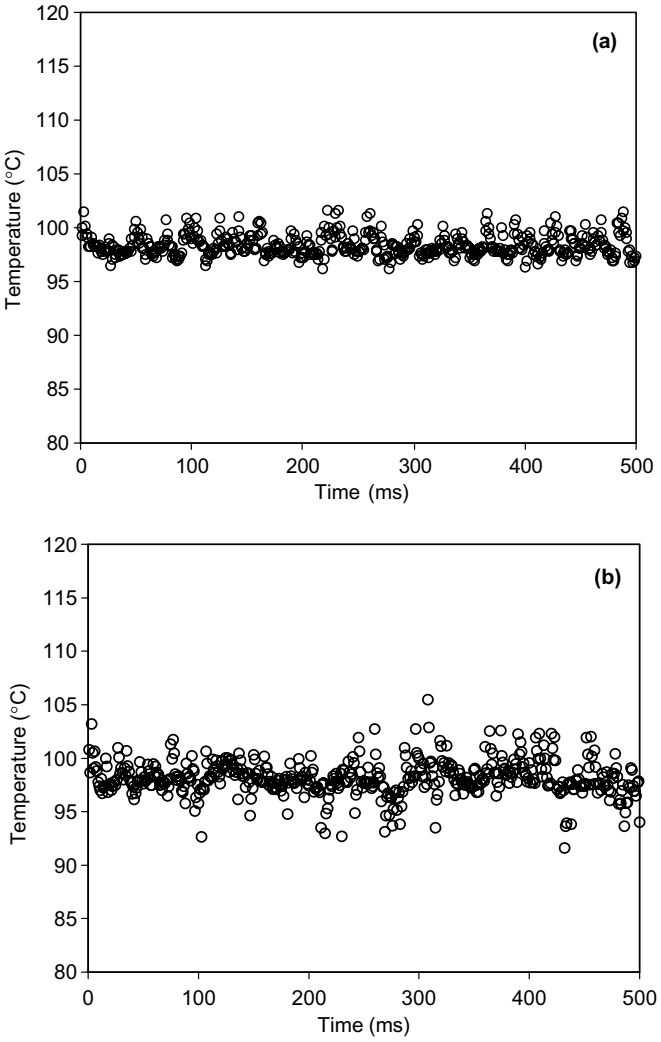


Fig. 13. Transients of the temperature at $d = 0$ mm (the upper surface) at (a) $w = 0$ mm and (b) $w = 4.5$ mm for a gap distance of 500 μm and a heat flux of 160 kW/m$^2$.

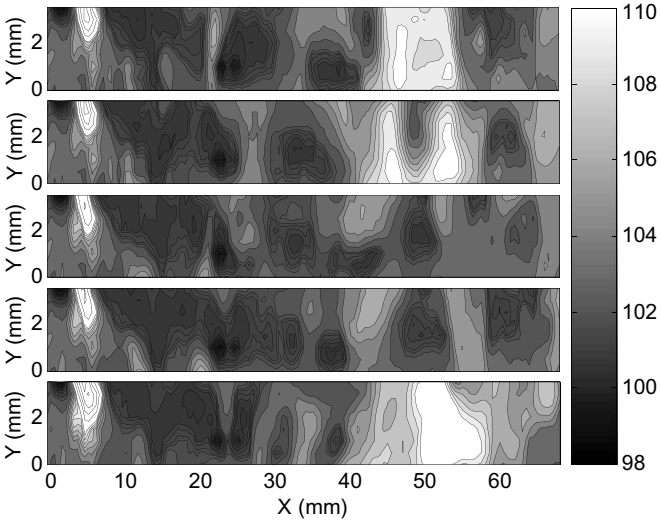


Fig. 14. Transients of instantaneous temperature distribution (°C) on the heated foil for a gap distance of 200 μm and a heat flux of 60 kW/m$^2$. These images were recorded 17 ms apart.

at the depth of 1 mm below the surface, suggesting that there was little vapour penetration at this depth in the porous media.

The instantaneous temperature distributions on the foil heater for a gap distance of 200 μm at a heat flux of 60 kW/m$^2$ are presented in Fig. 14. The temperature over most of the foil is relatively uniform even at this heat flux that approaches the largest value for stable operation. This behaviour is similar to the cases with large gap distances. However, there are also high temperature regions, with a maximum temperature exceeding 130 °C, more characteristic of the zero gap case. Thus, this gap distance, which is similar to the mean pore radius of the porous plate, does seem to represent a transition between the smaller and larger gap distance cases.

## 4. Conclusions

An experimental investigation was performed to examine the effect that the presence of a gap between a heated finned surface and a saturated porous plate has on the heat transfer between these surfaces. The maximum heat flux that could be achieved before there was a dramatic increase in the average surface temperature of the heated fin increased significantly as the gap distance was increased from 0 to 500 μm. The heat transfer performance remained relatively independent of the gap distance for distances between 500 and 900 μm.

Measurements of the instantaneous temperature on the heated surface and within the porous plate indicate that there was a change in the boiling dynamics when the gap distance between the heated surface and the porous plate exceeded approximately 200 μm. When the gap distance was smaller than this distance, the vapour appeared to periodically build up beneath the heated surface before being exhausted to the vapour grooves. This cyclic behaviour allowed for the stable operation of the evaporator despite the occurrence of local high temperature regions on the heated surface. For larger gap distances, the vapour did not appear to build up below the fin, but instead seemed to escape to the vapour grooves relatively easily. This seems to be responsible for the dramatic increase in the heat transfer performance of the finned heated surface when the gap was introduced between the heated surface and the porous plate. The transition gap distance was similar to the mean pore size suggesting that the optimal gap distance should be larger than the pore size as suggested by Platel et al. [15].

## Acknowledgements

The support of the Canadian Space Agency, Ontario Centres of Excellence and Acrolab Ltd is gratefully acknowledged. The first author would like to acknowledge the financial support from the National Sciences and Engineering Research Council (NSERC) of Canada through a PGS A scholarship. The authors would also like to thank

Dr. J.S. Chang and Mr. M. Khammar for their contributions to this work.

## References

[1] D. Butler, Overview of CPL and LHP Applications on NASA Missions, Space Technology and Applications International Forum. Albuquerque, NM. AIP Conference Proceedings 458 (1999) 792–798.
[2] P. Chen, W. Lin, The application of capillary pumped loop for cooling of electronic components, Appl. Therm. Eng. (21) (2001) 1739–1754.
[3] D. Liepmann, Design and fabrication of a micro-CPL for chip-level cooling, Proc.: 2001 ASME Int. Mech. Eng. Congress Exposition. (2001) 1–4.
[4] J. Ku, Operating characteristics of loop heat pipes, SAE Technical Paper 1999-01-2007, 1999.
[5] Y. Cao, A. Faghri, Conjugate analysis of a flat-plate type evaporator for capillary pumped loops with three-dimensional vapour flow in the groove, Int. J. Heat Mass Transfer (37) (1994) 109–401.
[6] Y. Cao, A. Faghri, Analytical solutions of flow and heat transfer in a porous structure with partial heating and evaporation on the upper surface, Int. J. Heat Mass Transfer (37) (1994) 1525–1533.
[7] E. Embacher, H.G. Wulz, Capillary pumped loops for space applications: experimental and theoretical studies on the performance of capillary evaporator designs, Proceedings of AIAA/ASME 5th Joint Thermophysics and Heat Transfer Conference, Seattle WA, AIAA-90-1739, 1990.
[8] D. Khrustalev, A. Faghri, Heat transfer in the inverted meniscus type evaporator at high heat fluxes, Int. J. Heat Mass Transfer (38) (1995) 3091–3101.
[9] A.S. Demidov, E.S. Yatsenko, Investigation of heat and mass transfer in the evaporation zone of a heat pipe operating by the inverted meniscus principle, Int. J. Heat Mass Transfer (37) (1994) 2155–2163.
[10] H.G. Wulz, F. Mayinger, Heat and fluid transport in an evaporative capillary pump, Int. J. Energy Res. (16) (1992) 879–896.
[11] T.S. Zhao, Q. Liao, A visual study of phase-change heat transfer in a two dimensional porous structure with a partial heating boundary, Int. J. Heat Mass Transfer (43) (2000) 1089–1102.
[12] Q. Liao, T.S. Zhao, Evaporative heat transfer in a capillary structure heated by a grooved block, AIAA J. Thermophys. Heat Transfer (13) (1999) 126–133.
[13] T.S. Zhao, Q. Liao, On capillary-driven flow and phase-change heat transfer in a porous structure heated by a finned surface: measurements and modeling, Int. J. Heat Mass Transfer (43) (2000) 1141–1155.
[14] C. Figus, S. Bories, M. Prat, Investigation and analysis of a porous evaporator for a capillary pumped loop, Eng. Syst. Des. Anal., ASME PD-vol. 78 (6) (1996) 99–106.
[15] V. Platel, O. Fudym, C. Butto, P. Briend, Heat transfer coefficient at vaporization interface of a two phase capillary pump, Revue Generale de Thermique (35) (1996) 592–598.
[16] V. Dupont, J.L. Joly, M. Miscevic, V. Platel, Capillary pumped loop startup: effects of the wick fit on boiling incipience, J. Thermophys. Heat Transfer (17) (2003) 138–144.
[17] J.L. Devore, Probability and Statistics for Engineering and the Sciences, fifth ed., Duxbury Thomsom Learning, Pacific Grove CA, 2000, p. 50.
[18] N. Gao, H. Sun, D. Ewing, Heat transfer to impinging round jets with triangular tabs, Int. J. Heat Mass Transfer (46) (2003) 2557–2569.